Int. J. Bio-Inorg. Hybr. Nanomater., 5(1): 19-26, Spring 2016

The effect of Silica coating on bioactivity and biodegradability of Hydroxyapatite synthesized in collagen matrix

M. Seyed Sadjadi[1*]; F. Najafizadeh[1]; S.G. Fateami[2]; M. Karimi Mobarakeh[3]; R. Malekpour Afshar[4]

[1] Department of Inorganic Chemistry, Science and Research Branch, Islamic Azad University, Tehran, Iran

[2] Department of Chemistry, Basic Sciences Faculty, Islamic Azad and Shahid Bahoonar University, Kerman, Iran

[3] Department of Trauma and Orthopedic Surgery, Kerman University of Medical Sciences, Kerman, Iran

[4] Department of Pathology, Medical School, P.O Box 444 Kerman University of Medical Sciences, Kerman, Iran

Received: 22 November 2015; Accepted: 25 January 2016

ABSTRACT: The aim of this work was to investigate the effect of silica coating on bioactivity and biodegradability of hydroxyapatite. In this purpose, we firstly attempted to synthesis hydroxyapatite (HA) nanoparticles and its silica coated (Si-HA) sample in collagen matrix using calcium chloride, sodium phosphate and sodium silicate. Characterization of the sample was carried out using Fourier transform infrared spectroscopy (FTIR), Scanning and transmission electron microscopy (SEM & TEM) and XRD patterns. The great decrease in HA's crystallinity observed in XRD pattern and grain size growth and morphological change of HA in silica coated samples after 72 hrs immersion in SBF solution was attributed to the bioactivity and bio-degradability of HA in silica coated samples.

Keywords: *Bioactivity; Bio-degradability; Collagen matrix; SBF solution; Silica coated hydroxyapatite*

INTRODUCTION

Today, hydroxyapatite, $Ca_{10}(PO4)_6(OH)_2$ and calcium phosphate based materials are being increasingly used as implants and synthetic bone grafts. Beside of the good bioactivity and osteoconductivity of these materials they are not osteogenic and active in bone regeneration. Therefore, they have to be associated with bone growth osteogenic factors, such as mesenchymal progenitor cells (Cancedda, *et al.*, 2007, Fischer, *et al.*, 2003, Mankani, *et al.*, 2001). In this condition, many problems in controlling the shape, size, and textural properties of the materials will be created at the presence of osteogenic bioactive molecules (Fischer, *et al.*, 2003, Mankani, *et al.*, 2001). Many attempts have been therefore undertaken worldwide to improve bone orthopaedic or dental implants fixation properties through the chemical surface modification. The main goal in this in this process was to achieve a faster bone growth and chemical bonding of the implant with the newly generated and bone. Some of the most signifi-

(*) Corresponding Author - e-mail: ms6118228@gmail.com

cant approaches for osseointegration and in tissue engineering of bone regeneration have been reviewed in a special issue of Science (Kiberstis, *et al.*, 2000). A major improvement in this area has been achieved by addition of surface modified calcium hydroxyapatite (HA) with silica/silicate species. A successful work have been reported by Biomaterials group at Cambridge University (Prof Bill Bonfield) using high concentrated silica (30–50 wt.%) containing materials, such as bioglasses and glass-ceramics (Sun, *et al.*, 2001, Hench and Polak, 2008, Yuan, *et al.*, 2001). They also have developed a silicon substituted (0.8 wt.%) HA in granular form. More recently enhanced nucleation or fast formation of bone like layer of HA nanocrystals at the surface of TCP nanoparticles in a simulated body fluid solutions containing sodium silicate has been reported by us (Sadjadi, *et al.*, 2011). We have demonstrated that, surface modification of hydroxyl apatite by SBF solution containing sodium silicate can successfully promote bone marrow stem cell growth in 7 days (Sadjadi, *et al.*, 2010). Herein, for better understanding about silica coated and silica substitute HA and their influence on the human osteoblast-proliferation behavior (an in vivo study), we firstly attempted to synthesize silica coated hydroxyapatite nonocomposite (Si-HA) by a sample method. Characterization of the samples prepared in this stage revealed a great change in the sample's morphology and decrease of nHA crystallinity after its immersion in silica solution. These results can be attributed to the highest bioactivity and bio-degradability of the silica coated nHA samples.

MATERIALS AND METHODS

Materials

All chemicals regents, collagen, $CaCl_2.2H_2O$, $Na_3PO_4.12H_2O$, NH_3 and NH_4Cl, were supplied from Merck company and used without any further purifications. Infrared Spectroscopy (FTIR; Thermo Nicolet Nexus 870), Scanning Electron Microscopy (SEM; Philips electron microscope) and Transmission Electron Microscope (TEM; Philips EM208 and microscope operated at 100 kV) and X-ray Powder diffractometry (XRD; Seisert Argon 3003 PTC using nickel-filtered XD-3D Cu Ka radiations (λ = 0.154 nm) were used for characterization of the samples.

Synthesis of hydroxyapatite nanocomposites

The procedure for preparation of the samples was the same as described by (Lo pez-Alvarez, *et al.*, 2009) with some small modification. Firstly 1.2, 2.8 and 4g of collagen was dissolved in 70 mL of distilled water and stirred continuously by a magnetic stirrer in its maximum speed and heated simultaneously at about 68°C. After stirring for 2 hours, 80 mL of calcium chloride solution (0.1 M) was slowly added to the above prepared biopolymer solution. After stirring for 1 hour, 48 mL of sodium phosphate (0.1 M) was added drop wisely, and stirred again under controlled pH = 10. The products obtained were finally filtered and washed with double-distilled water to eliminate sodium chloride as by product, and dried at room temperature.

Table 1. Inorganic constituents for preparation of 1000 mL of SBF solution.

Order	Reagent	Amount	Container	Purity (%)	Formula weight
1	NaCl	8.035g	Weighting paper	99.5	58.4430
2	$NaHCO_3$	0.355g	Weighting paper	99.5	84.0068
3	KCl	o.225g	Weighting bottle	99.5	74.5515
4	$K_2HPO_4.3H_2O$	0.231g	Weighting bottle	99.0	228.2220
5	$MgCl_2.6\ H_2O$	0.311g	Weighting bottle	98.0	203.3034
6	1.0M HCl	39 mL	Graduated cylinder	-	-
7	$CaCl_2$	0.292g	Weighting bottle	95.0	110.9848
8	Na_2SO_4	0.072g	Weighting bottle	99.0	142.0428
9	Tris	6.118g	Weighting paper	99.0	121.1356
10	1.0M HCl	0 – 5 mL	Syringe	-	-

Table 2. Ion concentrations of SBF in comparison with those in human blood plasma.

Ion	Ion concentrations (m M)	SBF
	Blood Plasma	
Na^+	142.0	142.0
K^+	5.0	5.0
Mg^{2+}	1.5	1.5
Ca^{2+}	2.5	2.5
Cl^-	103.0	147.8
$HCO3^-$	27.0	4.2
$HPO4^{2-}$	1.0	1.0
$SO4^{2-}$	0.5	0.5
pH	7.2 – 7.4	7.40

Synthesis of siliceous hydroxyapatite nanocomposite

Siliceous hydroxyapatite nanocomposite was prepared by dispersing above prepared nanocomposite in 30 cc of double-distilled water containing 7.0g Na_2SiO_3 in a beaker and stirred for 24 hours at the room temperature. The sample was then incubated for 72 hours at 36.5°C and the product was filtered and washed with double-distilled water, and dried at room temperature.

Preparation of SBF solution

The SBF solution was prepared according the method described by (Kokubo and Takadama, 2006). According to this approach, for preparation of 1000 mL of SBF solution, 700 mL of distilled water in a 1000 mL plastic beaker was heated to 36.5 ± 1.5°C under stirring and the reagents of No. 1 to 8 (given in Table 1), was dissolved one by one into the solution at (36.5 ± 1.5°C). The reagents of No. 9 (Tris as buffering agent) and No.10 (small amount of molar HCl) were finally added for pH adjustment to 7.4 and finally we added distilled water up to 900 mL in total. When the solution temperature falls to 20°C, we adjusted the solution volume to 1000 mL by adding distilled water. The nominal ion concentrations of SBF solution in comparison with those of human blood plasma is shown in Table 2.

RESULTS AND DISCUSSION

FTIR study

Fig. 1a,b represents FTIR spectra of the as prepared nHA in collagen matrix before and after immersion in sodium silicate solution. In these spectra, characteristic absorption bands appearing at 561, 603 and 986-1100 cm^{-1} show the presence of functional phosphate groups for both the cases even after immersion in SBF solution (Kokubo and Takadama, 2006). Furthermore, the peaks observed at 3571 and 1640 cm^{-1} were due to vibrational bands of hydroxyl group (Lopez-Alvarez, *et al.*, 2009, Russell, *et al.*, 1996). This observation confirms the presence of phosphate groups in the samples before and after immersion in silica solution. After immersion of the HA firstly in silica-containing solution and then in SBF solution for 72 hrs, three new small peaks in comparison with HA spectra have been appeared.

They were peaks at 471 cm^{-1} (υ_1), 798 cm^{-1} (υ_2), and 1210 cm^{-1} (υ_3), as shown in the spectra after immersion in SBF solution. The bands at 417 cm^{-1} and the shoulder at 1210 cm^{-1} have been assigned to Si–O–Si bending mode and the band at 798 cm^{-1} can be related to the Si–O–Ca vibration band (YingJun, *et al.*, 2006, Xia and Chang, 2007). These results, can be related to the formation of a silicate apatite (Si-HA) (Sinha and Guha, 2008) on the surface of as synthesized HA. Note that, absorption bands observed in the range of 1300–1650 cm^{-1} have been assigned to the stretching and bending modes of C–O and P–O bonds and air carbonated $(CO_3)^{2-}$ ions (Gou and Chang, 2004, Toworfe, *et al.*, 2006, Wang, *et al.*, 2002, Rehman and Bonfield, 1997).

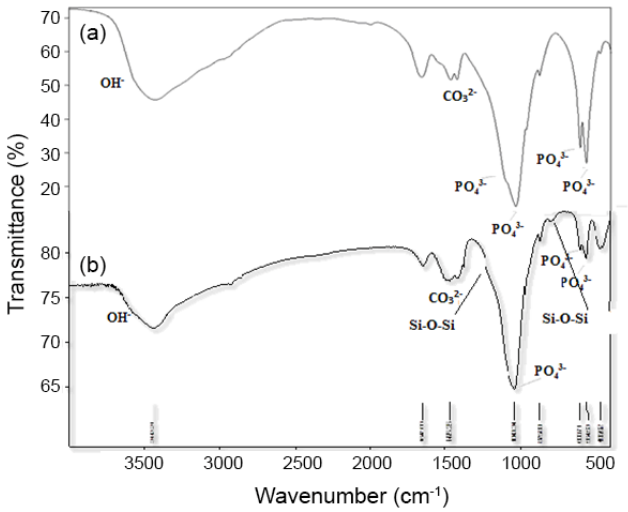

Fig. 1. FTIR spectra of : a) nHAp; b) silica coatted nHA nanocomposites. This Figure illustrates the hdroxy apatite's characteristic absorption bands in both the cases.

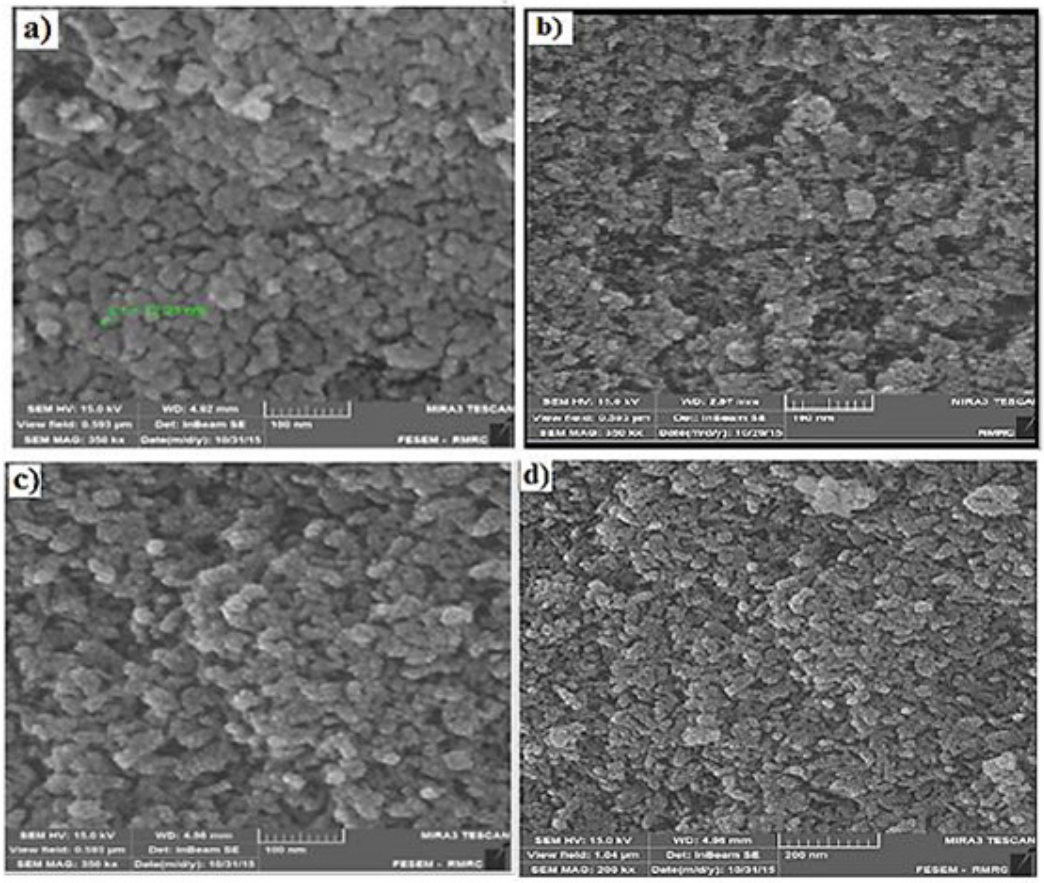

Fig. 2. SEM image of nHAp synthesized in: a) 1.2; b) 2.8 and c,d) 4 gram collagen matrix.

Morphological study

Scanning electron microscopy (SEM)

Fig. 2a-d represents SEM images of the HA prepared in 1.2, 2.8, and 4 gram collagen matrix. A simple comparison of these images reveals that, the smaller nanocrystallite or nanorods has been formed for the sample containing 4 gram collagen as a matrix.

Fig. 3a,b, shows SEM images of the as synthesized nHA in 2.8 g collagen before and after immersion in SBF solution. Growth and redistribution of HA nanocomposte after its immersion in SBF solution can be easily observed in Fig. 3b.

Fig. 4a,b and Tables 3,4 represent dispersive analysis of X-ray (EDAX) results obtained for HA and sil-

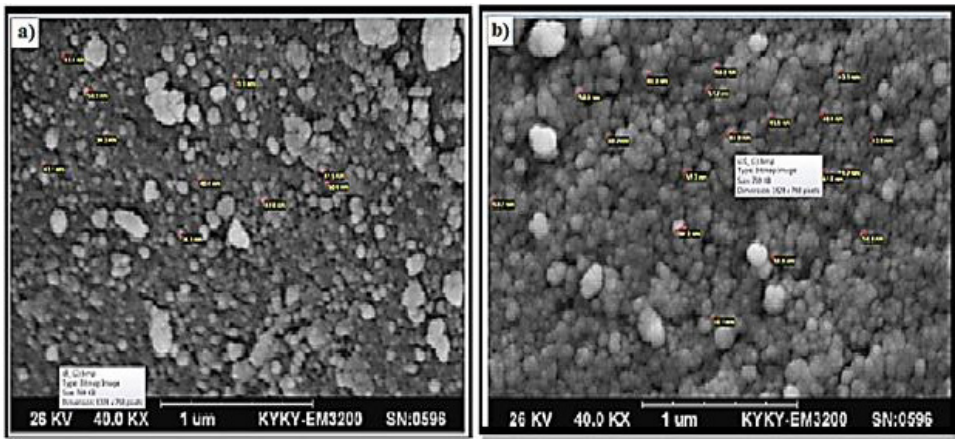

Fig. 3. SEM image of nHA synthesized in 2.8 g collagen: a) before and b) after 72 hrs immersion in SBF solution.

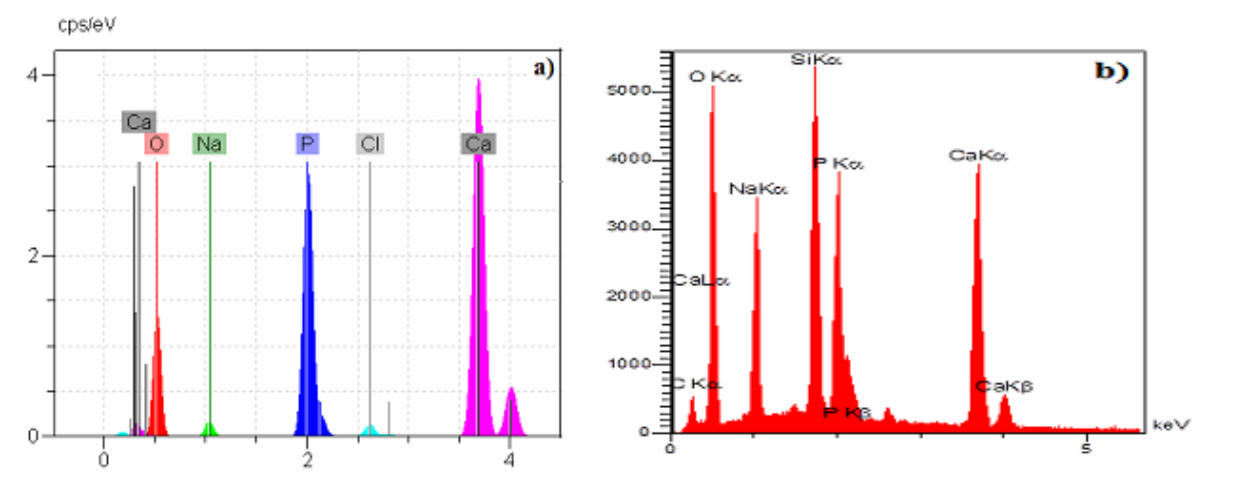

Fig.4. X-ray dispersive analysis results (EDAX) for: a) HA synthesized in this work; b) Siliceous HA nanocomposites.

Table 3. EDAX ZAF Elemental quantification of the as prepared HAp.

Element	Series	Unn. C (Wt.%)	Nrm. C (Wt.%)	Atom. C (At.%)
O	K	31.61	28.00	46.73
Na	K	1,72	1.53	1.77
P	K	25.71	22.78	19.63
Cl	K	1.15	1.02	0.76
Ca	K	52.68	46.68	31.10

Table 4. EDAX ZAF Elemental quantification of prepared silica coated nHAp.

Element	Series	Unn. C (Wt.%)	Nrm. C (Wt.%)	Atom. C (At.%)
C	K	10.36	7.40	16.68
O	K	48.24	80.94	58.27
Na	K	5.69	10.11	4.79
Si	K	8.70	20.80	5.99
P	K	8.88	18.99	5.54
Ca	K	18.13	37.24	8.74

ica coated HA nanocomposites. These results shows that, the average Ca/P atomic ratio was at about 1.58 in both the cases and confirm therefore that, the silica substitution in HA structure has not been occurred.

Transmission electron microscopy (TEM)

Fig. 5a,b show the TEM images of nHA synthesized in 2.8 gram collagen as a matrix before and after immersion in the sodium silicate solution. Formation of rod like nHAp shown in Fig. 5a, with 35 nm long and 5.5 nm diameters in the presence of collagen matrix can be observed. In figure 1b silica coated nHA nanoparticles after immersion of HA in sodium silicate was shown.

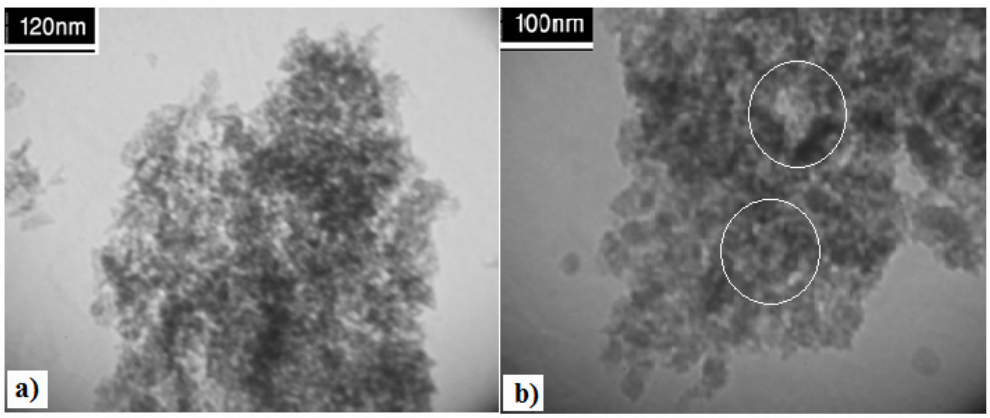

Fig. 5a,b. TEM image of: a) nHAp synthesized in 2.8 g collagen matrix before and (b) after silica coating.

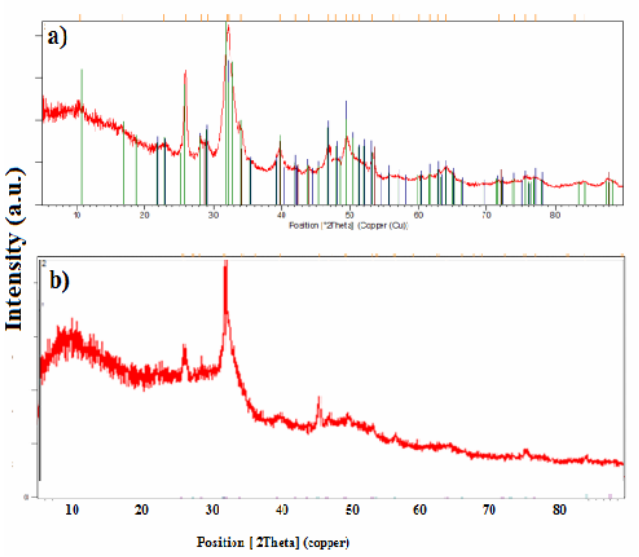

Fig. 6. Powder X-ray diffraction of: a) nHAp; Silica coated HA nanocomposites after 72 hrs immersion in SBF solution.

XRD study

Fig. 6a,b shows powder X-ray diffraction patterns of the prepared nHAp and Si-nHA after soaking 72 h in SBF solution at 37°C. The diffraction peaks appearing in the Fig. 6a was identified using PDF card # 00-024-0033 as well as 00-001-1008 and 00-009-0432 concerning to the hexagonal HA structure. In this pattern, all the major peaks were the same as recorded for XRD pattern of hexagonal HA (P63/m). The diffraction peaks of Si-nHA shown in the Fig. 6b was identified to PDF card # 00-001-0008 corresponding to the Calcium Hydroxide Phosphate, $Ca_{10}(PO4)_6.(OH)_2$ with some impurity peaks corresponding to NaCl. Interesting point in this pattern was absence of the peaks concerning to the silica crystallites. Only a broad and relatively intense peak appeared at low angle which may be due to amorphous silica presence.

Noting that, the highest diffraction peak for both the cases at 2θ values of 32.24 and 32.197 corresponding to (112) Miller plane was selected for calculation of crystalline size. The mean crystallite size (D) for both the prepared samples was therefore calculated from the XRD line broadening measurement using Scherrer equation:

$$D = \frac{0.89\lambda}{\beta \cos\theta}$$

Where, λ is the wavelength (Cu; Kα), β is the full width at the half maximum of HA (112) line and θ is the diffraction angle. The average crystallite size, calculated for HA samples after 72hrs soaking in SBF solution was 5.6 nm. A closer look at these HA patterns shows occurrence of a major change or decrease in HA structure crystallinity in revenge to the formation of a glassy form of HA due to the silica coating in Si-HA samples was and can be attributed to the highest bioactivity; bio-degradability of the HA samples and formation of simultaneous silica and HA in a glass form during the 72 hrs immersion of the Si-HA samples in SBF solution.

CONCLUSIONS

- The presence of PO_4^{3-} group in both the HA and Si-HA synthesized in collagen matrix confirmed by characteristic FTIR absorption peaks of PO_4^{3-}.
- Formation of HA framework in both the cases (HA and Si-HA) has been confirmed by XRD patterns and appearance of the FTIR characteristic stretching vibration of OH- groups in HA structure at 3575 cm^{-1} .
- The EDAX elemental analysis data and appearance of two new additional bands at 798 and 1210 cm^{-1} confirm presence of silica derivatives in Si-HA samples.
- The same atomic ratio of Ca/P observed from the EDAX elemental analysis data for the HA samples before and after immersion in silica solution confirms that no substitution of the phosphate groups by silicate ions has been occurred in Si-HA samples.
- Decrease of HA's crystallinity in Si-HA sample and formation of a glassy form of HA in revenge and growth of its grain size after 72 hrs immersion in SBF solution can be attributed to the bioactivity and biodegradability of HA in silica coated samples.

ACKNOWLEDGEMENT

The financial and encouragement support provided by the Research vice Presidency of Tehran Science and Research Branch, Islamic Azad University and Iranian Nanotechnology Initiative (Govt. of Iran).

REFERENCES

Cancedda, R., Giannoni, P., Mastrogiacomo, M.A., (2007). Tissue engineering approach to bone repair in large animal models and in clinical practice. Biomaterial, 28: 4240–4250.

Fischer, E.M., Layrolle, P., Van Blitterswijk, C.A., De Bruijn, J.D., (2003). Bone formation by mesenchymal progenitor cells cultured on dense and microporous hydroxyapatite particles. Tissue Eng., 9: 1179–1188.

Mankani, M.H., Kuznetsov, S.A., Fowler, B., Kingman, A., Robey. P.G., (2001). In vivo bone formation by human bone marrow stromal cells: Effect of carrier particle size and shape. Biotechnol Bioeng., 72: 96–107.

Kiberstis, P., Smith, O., Norman C., (Eds.), (2000). Bone health in the balance. Science, 289: 1497–1514.

Sun, L., Berndt, C.C., Gross, K.A., Kucuk, A., (2001). Material fundamentals and clinical performance of plasma-sprayed hydroxyapatite coatings: a review. J. Biomed. Mater. Res., 58: 570-579.

Hench, L.L., Polak, M.J., (2008). A Genetic Basis for Design of Biomaterials for In Situ Tissue Regeneration. Key Eng. Mater., 377: 151–166.

Yuan, H., De Bruijn, J.D., Zhang, X., Van Blitterswijk, C.A., De Groot, K., (2001). Bone induction by porous glass ceramic made from Bioglass (45S5). Biomed. Mater. Res. A, 58: 270-276.

Sadjadi, M.S., Ebrahimi, H.R., Meskinfam, M., Zare, K., (2011). Silica enhanced formation of hydroxyapatite nanocrystals in simulated body fluid (SBF) at 37◦C, Mate. Chem. Phys., 130: 67– 71.

Sadjadi, M.S., Meskinfam, M., Sadeghi, B., Jazdarreh, H., Zare, K., (2010). In situ biomimetic synthesis, characterization and in vitro investigation of bone-like nanohydroxyapatite in starch matrix, Mater. Chem. Phys., 124: 217–222.

Kokubo, T., Takadama, H., (2006). Leading Opinion, How useful is SBF in predicting in vivo bone bioactivity, Biomaterial, 27: 2907–2915.

Lopez-Alvarez, M., Solla, E.L., Gonzalez, P., Serra, J., Leon, B., Marques, A.P., Reis, R.L., (2009). Silicon-hydroxyapatite bioactive coatings (Si-HA) from diatomaceous earth and silica, Study of adhesion and proliferation of osteoblast-like cells, J. Mater. Sci. Mater. Med., 20: 1131–1136.

Russell, S.W., Luptak, K.A., Suchicital, C.T.A., Alford, T.L., Pizziconi, V.B., (1996). Chemical and Structural Evolution of Sol-Gel-Derived Hydroxyapatite Thin Films under Rapid Thermal Processing. J. Am. Ceram. Soc., 79: 837-842.

YingJun, W., JingDi, C., Kun, W., Zhang, S.H., Xidong, W., (2006). Surfactant-assisted synthesis of hydroxyapatite particles. Mater. Lett., 60: 3227-3231.

Xia, W., Chang, J., (2007). Preparation and characterization of nano-bioactive-glasses by a quick alkali mediated sol-gel method. Mater. Lett., 61: 3251-3253.

Sinha, A., Guha, A., (2008). Biomimetic patterning of polymer hydrogels with hydroxyapatite nanoparticles, Mater. Sci. Eng. C, 29: 1330-1333.

Gou, Z., Chang, J., (2004). Nodule formation and mineralisation of human primary osteoblasts cultured on a porous bioactive glass scaffold. J. Eur. Ceram. Soc., 24: 3491-3497.

Toworfe, G.K., Composto, R.J., Shapiro, I.M., Ducheyne, P., (2006). Nucleation and growth of calcium phosphate on amine-, carboxyl- and hydroxyl-silane self-assembled monolayers. Biomaterial, 27: 631-642.

Wang, X., Li, Y., Wei, J., de Groot, K., (2002). Development of biomimetic nano hydroxyapatite/poly(hexamethylene adipamide) composites. Biomaterial, 23: 4787-4791.

Rehman, I., Bonfield, W., (1997). Characterization of hydroxyapatite and carbonated apatite by photo acoustic FTIR spectroscopy. J. Mater. Sci. Mater. Med., 8: 1-4.

AUTHOR (S) BIOSKETCHES

Mirabdullah Seyed Sadjadi, Professor, Department of Inorganic Chemistry, Science and Research Branch, Islamic Azad University, Tehran, Iran, *E-mail: ms6118228@gmail.com*

Fariba Najafizade, Ph.D., Department of Inorganic Chemistry, Science and Research Branch, Islamic Azad University, Tehran, Iran

Seyed Jemiladine Fateami, Ph.D., Department of Chemistry, Basic Sciences Faculty, Islamic Azad and Shahid Bahoonar University, Kerman, Iran

Mahmood Karimi Mobarakeh, Ph.D., Department of Trauma and Orthopedic Surgery, Kerman University of Medical Sciences, Kerman, Iran

Mahmood Karimi Mobarakeh, Ph.D., Department of Pathology, Medical School, P.O Box 444 Kerman University of Medical Sciences, Kerman, Iran